Channel Plasmon-Polariton Guiding by Subwavelength Metal Grooves

Sergey I. Bozhevolnyi,[1,*] Valentyn S. Volkov,[1] Eloïse Devaux,[2] and Thomas W. Ebbesen[2]

[1]*Department of Physics and Nanotechnology, Aalborg University, Pontoppidanstræde 103, DK-9220 Aalborg Øst, Denmark*
[2]*Laboratoire des Nanostructures, ISIS, Université Louis Pasteur, 8 allée Monge, BP 70028, 67083 Strasbourg, France*

(Received 4 February 2005; published 22 July 2005)

We report on realization of channel plasmon-polariton (CPP) propagation along a subwavelength metal groove. Using imaging with a near-field microscope and end-fire coupling with a tapered fiber connected to a tunable laser at telecommunication wavelengths (1425–1620 nm), we demonstrate low-loss (propagation length $\sim 100\ \mu$m) and well-confined (mode width $\cong 1.1\ \mu$m) CPP guiding along a triangular 0.6 μm-wide and 1 μm-deep groove in gold. We develop a simple model based on the effective-index method that accounts for the main features of CPP guiding and provides a clear physical picture of this phenomenon.

DOI: 10.1103/PhysRevLett.95.046802 PACS numbers: 73.20.Mf, 07.79.Fc, 71.36.+c

Surface plasmon polaritons (SPPs) are quasi-two-dimensional electromagnetic excitations, propagating along a dielectric-metal interface and having the field components decaying exponentially into both neighboring media [1]. SPPs are tightly bound to the metal surface penetrating on ~ 100 nm in dielectric and ~ 10 nm in metal, a feature that implies the possibility of using SPPs for miniature photonic circuits and interconnects [2]. The main issue in this context is to strongly confine the SPP field in the cross section perpendicular to the SPP propagation direction (smaller cross sections ensure smaller bend losses and higher densities of components), while keeping relatively low propagation losses. It has been shown using numerical simulations that nanometer-sized metal rods can support extremely confined SPP modes propagating though only over hundreds of nanometers [3]. Similar properties were expected [4] and indeed found [5] for the electromagnetic excitations supported by chains of metal nanospheres. SPP propagation along metal stripes [6] and channels in periodically corrugated regions [7] has also exhibited propagation losses increasing drastically with the decrease in the stripe/channel width. Quite recently, SPP gap waveguides based on the SPP propagation between metal surfaces with varying separation [8] or material properties [9] have been suggested. It should be noted that, in general, the SPP confinement is achieved primarily by decreasing the SPP spatial extent into dielectric, thereby increasing the portion of SPP power being absorbed by metal, so that the choice of optimum guiding configuration is subject to trade-off with many intricate issues yet to be elucidated.

The possibility of radiation guiding by a channel cut into a planar surface of a solid (metal or polar dielectric) characterized by a negative dielectric function was first considered by Maradudin and co-workers, first (nearly 15 years ago) in the electrostatic limit [10] and later on with retardation being taken into account [11]. In the latter work, the channel guided waves were termed as channel polaritons (CPs), and most of the results were reported for a real negative dielectric function, i.e., in the absence of absorption, but it has been suggested there that the CP propagation length should be comparable to that of SPP on a planar metal surface. Very recently, the CP propagation in triangular (V) grooves on a metal substrate has been numerically investigated, considering first infinitely deep V grooves (and corroborating the previous findings for curved grooves) [12] and, afterward, finite-depth V grooves so as to realize the single-mode CP guiding [13]. In these reports, it has also been pointed out that the channel plasmon polaritons (CPPs) exhibit superior features for subwavelength guiding, such as relatively low propagation losses for strongly confined CPPs, broadband transmission, and compatibility with the planar technology.

Here we report what we believe to be the first realization and characterization of CPP propagation along a subwavelength-sized metal groove. We suggest also a simple model that accounts for the main features of CPP guiding by metal grooves and provides a clear physical picture of this phenomenon.

Let us first briefly review the properties of SPPs guided inside narrow slits between two metal surfaces. For an individual metal surface, the SPP propagation constant β is given by $\beta = (2\pi/\lambda)[\varepsilon/(\varepsilon + 1)]^{0.5}$, where λ is the wavelength in air and ε is the metal dielectric constant [1]. The real part of β can be related to the SPP effective refractive index, i.e., $N_{\mathrm{eff}} = (\lambda/2\pi)\,\mathrm{Re}\,(\beta)$, whereas its imaginary part determines the SPP propagation length: $L = [2\,\mathrm{Im}\,(\beta)]^{-1}$. For two close metal surfaces, the SPPs associated with individual metal surfaces become coupled, and the dispersion relation for β becomes implicit [9] though its solution can be readily obtained [8,9]. Hereafter, we consider only a symmetric combination of the individual SPPs, so that its magnetic field component maintains the sign across the slit. The effective index of this slit SPP (S-SPP) as a function of the slit width is shown in Fig. 1 along with the S-SPP propagation length for silver (for $\lambda = 0.633\ \mu$m and $\varepsilon_s = -16.22 + 0.52i$ [13]) and

 © 2005 The American Physical Society

gold (for $\lambda = 1.55$ μm and $\varepsilon_g = -132 + 12.65i$ [14]) surfaces. The first set of parameters corresponds to that used previously in modeling of CPPs by means of the finite-difference time-domain algorithm [12,13], whereas the second one is related to that investigated experimentally and reported here. It is seen that, with the decrease of the slit width, the S-SPP effective index increases while the S-SPP propagation length decreases, both starting from the values corresponding to the (individual) SPP.

The next step is to examine a straight groove cut into metal and having a cross section, whose width is monotonically decreasing with the increase of the depth. Since light tends to be confined in regions with higher refractive indexes, sufficiently deep grooves should support bound modes formed by S-SPPs that are confined to the groove bottom, where the S-SPP effective index is at maximum. This conclusion can be further verified and quantified, e.g., by making use of the effective-index (EI) approximation, which is one of standard approaches used for waveguide analysis in photonics [15]. We found it suitable also for modeling of long-range SPPs guiding by metal stripes [16]. In this approach, a two-dimensional guiding geometry is dealt with by treating (successively) two one-dimensional configurations. Thereby, one can find the groove-guided SPP mode, i.e., the CPP, by analyzing a one-dimensional layered (in depth) guiding structure, in which the top layer of air and the bottom layer of metal abut a stack of layers having refractive indexes determined by the layer depth: an index is equal to the S-SPP effective index for a slit width corresponding to the groove width at this depth.

We have first applied the EI method to the configuration analyzed previously [12,13] in order to verify its applicability for analyzing CPPs. Thus, we considered a silver V groove with the groove angle of 30° (at $\lambda = 0.633$ μm) using the width dependence of the S-SPP effective index shown in Fig. 1. We have found that the 314 nm-deep groove supports a single CPP mode with the effective index of $\cong 1.13$ (wave number $q \cong 1.12 \times 10^7$ m^{-1}) and the propagation length of $\cong 8.4$ μm. With the increase of the groove depth, the second CPP mode emerges at the groove depth of 0.78 μm. It was further found that, at the groove depth of 1.44 μm, the two CPP modes have the effective indexes of $\cong 1.15$ and 1.04 ($q \cong 1.14$ and 1.03×10^7 m^{-1}). We have also observed that the fundamental CPP mode index increases while the propagation length decreases with the decrease of the groove angle. The above results are in good *quantitative* agreement with those reported previously [12,13].

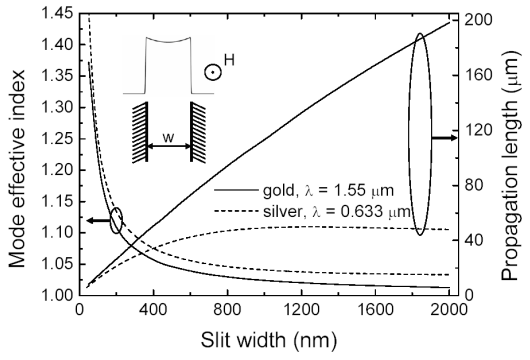

FIG. 1. The S-SPP (symmetric) mode effective index and its propagation length as a function of slit width w for gold (at the light wavelength $\lambda = 1.55$ μm) and silver ($\lambda = 0.633$ μm). The inset shows the slit configuration and S-SPP magnetic field orientation along with the example of S-SPP field distribution across a 1 μm-wide gold slit ($\lambda = 1.55$ μm).

Having confirmed the applicability of the EI method, we analyzed the CPP guiding at $\lambda = 1.55$ μm in gold V grooves (Fig. 2). Similarly to the above configuration, the CPP effective index increases while the propagation length decreases with the decrease of the groove angle θ. Note that the CPP mode index N_{eff} determines the mode confinement, since the mode penetration depth in air (above the sample surface) is given by $d_{\text{pen}} = (\lambda/2\pi) \times (N_{\text{eff}}{}^2 - 1)^{-0.5}$, so that a larger effective index corresponds to a smaller penetration depth and thereby better field confinement in depth (in width, the CPP mode is confined within the groove walls). Furthermore, the CPP propagation length starts to rapidly increase when the groove depth decreasing approaches a certain (cutoff) value. Since, at the same time, the CPP effective index approaches that of air, the increase of propagation length signifies the tendency of the CPP mode field being extended progressively outside the groove. Note that the existence of the cutoff depth for the fundamental CPP mode has not been pointed out in the previous reports [10–13]. It should also be mentioned that, in Fig. 2, the CPP characteristics are shown in the range of groove depths corresponding to the single-mode CPP guiding in the groove with the angle $\theta = 25°$.

For our experiments on CPP guiding, two $\sim$460 μm-long grooves have been fabricated (using a focused ion-beam milling technique) in a 1.9 μm-thick gold layer deposited on a substrate of fused silica covered with an 80 nm-thick indium-tin-oxide layer [Figs. 3(a) and 3(b)]. The groove profiles turned out being similar to triangular profiles, especially for groove N2. It is also

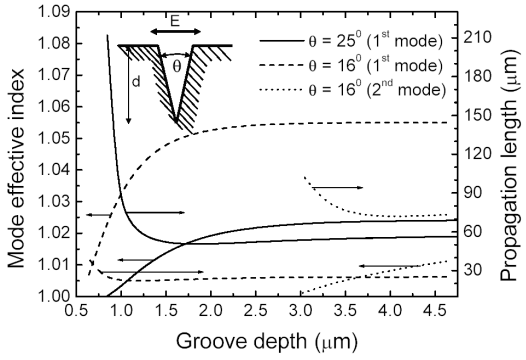

FIG. 2. The effective indexes of CPP modes and their propagation lengths as a function of groove depth d for different groove angles θ. The inset shows the groove configuration and dominant orientation of CPP electric field [17].

seen that the groove walls are somewhat rough, a feature that can influence the CPP propagation by causing the CPP scattering out of the groove. The widths and depths were measured as $w \sim 0.5$ and 0.6 μm and $d \sim 0.9$ and 1 μm for grooves N1 and N2, respectively. We have also evaluated the angles at the groove bottoms as $\theta \sim 16°$ and 25°. Taking into account limitations of the EI approximation and inaccuracies in the groove characterization, we concluded that both grooves support only the fundamental CPP mode and that groove N2 can be close to cutoff.

The experimental setup employed for the CPP observation and characterization is essentially the same as that used in our experiments with photonic crystal waveguides [17]. It consists of a collection scanning near-field optical microscope (SNOM) with an uncoated fiber tip used as a probe and an arrangement for launching tunable (1425–1620 nm) TE/TM-polarized (the electric field is parallel/perpendicular to the sample surface plane) radiation into a groove by positioning a tapered-lensed polarization-maintaining single-mode fiber [Fig. 3(c)]. The adjustment of the in-coupling fiber was accomplished when monitoring the light propagation along the surface with help of a far-field microscopic arrangement. The idea was to judge upon the CPP excitation and propagation by observing its scattering out of the surface plane by groove imperfections. We have found that the track of radiation propagating along a groove was visible only with groove N2 and only for TE polarization of incident light [Fig. 3(d)]. This track was clearly distinguishable for distances of up to $\sim$300 μm from the in-coupling groove edge and in the whole range of laser tunability.

The far-field observations have confirmed the expected polarization properties of the guided radiation [18] and demonstrated its (relatively) low dissipation. Following these experiments (that include also adjusting the in-coupling fiber position to maximize the coupling efficiency) we moved the whole fiber-sample arrangement under the SNOM head and mapped the intensity distribution near the surface of groove N2 with the SNOM fiber tip. The tip was scanned along the sample at a constant distance of a few nanometers maintained by shear force feedback, and the radiation collected by the fiber was detected with a femtowatt InGaAs photo receiver. Topographical and near-field optical images of efficient CPP guiding by groove N2 were recorded at the distance of $\sim$200 μm from the in-coupling groove edge (to decrease the influence of stray light, i.e., the light that was not coupled into the CPP mode) and in the whole range of laser tunability (Fig. 4). Appearance of the optical images is similar to those obtained with photonic crystal waveguides [17] featuring efficient mode confinement (in the cross section) at the groove and intensity variations along the propagation direction (Fig. 5). The latter can be most probably accounted for by the interference between the CPP mode and scattered (including stray light) field components [17]. However, the preliminary analysis of the spatial spectra for different wavelengths has shown that the situation is quite complicated, because these spectra exhibit several features that are independent on the light wavelength and might be related to the roughness of groove walls [Fig. 3(b)]. Leaving the detailed analysis of this phenomenon for future studies, we would like to mention that, despite the aforementioned signal variations, we could characterize the average full-width-at-half-maximum (FWHM) of the CPP mode and its propagation length (Fig. 5). It turned out that, in the wavelength range of 1425–1620 nm, the FWHM is practically constant (1.15 ± 0.1 μm) whereas the CPP propagation length (determined from the 36 μm-long SNOM images) was varying between $\sim$90 and 250 μm, depending on both the coupling arrangement and wavelength used. Since the gold dispersion alone is too small to account for these variations, we

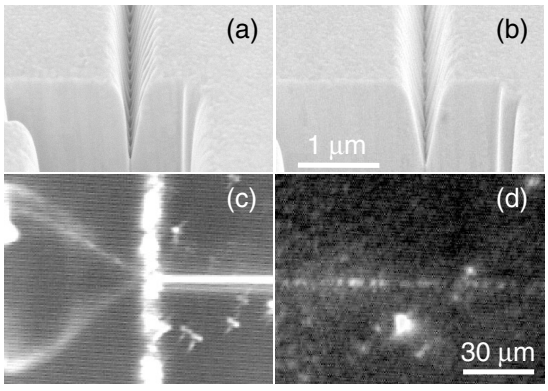

FIG. 3. Scanning electron microscope images of grooves (a) N1 and (b) N2. Optical microscope images of (c) the coupling arrangement (the tapered fiber is seen to the left and the illuminated groove to the right) and (d) the light propagation ($\lambda = 1.55$ μm) along groove N2 (from left to right) at a distance of $\sim$200 μm from the in-coupling groove edge.

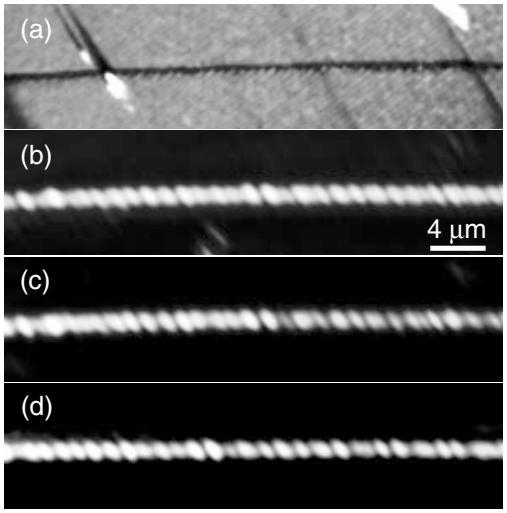

FIG. 4. Grayscale (a) topographical and near-field optical images (36×9 μm^2) taken with groove N2 at $\lambda \cong$ (b) 1.44, (c) 1.5, and (d) 1.57 μm. The CPP propagation is from left to right.

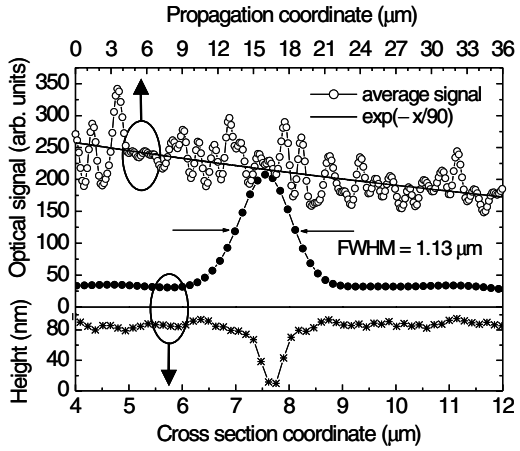

FIG. 5. Cross sections of the topographical (stars) and near-field optical (filled and open circles) images of Fig. 4 [Figs. 4(a) and 4(c), respectively] averaged along 10 lines along the propagation direction or perpendicular to it. The exponential dependence fitted by the least-square method to the signal dependence along the propagation direction is also shown.

attribute those to poor reproducibility of the fiber coupling that was adjusted using far-field observations [Fig. 3(d)] and that strongly influences the contribution to the detected signal from the scattered radiation. It should be noted that we have also recorded optical images in constant plane mode at the height of ~200 nm above the sample surface. These images exhibited only low-contrast noiselike signal variations with the average level of ~20% from the maximum signal associated with the CPP mode, confirming that the main contribution to the signal detected at the groove (Fig. 4) originates indeed from the CPP (evanescent) field.

The experimental observations reported above are consistent with the preceding discussion of the main properties of CPP modes. Considering groove N2 ($d \sim 1$ μm and $\theta \sim 25°$), it is expected that the fundamental CPP mode can be quite close to cutoff (Fig. 2). This means that its propagation length can easily be close to 100 μm or even longer, with the CPP field extending out of the groove. The latter would facilitate its observation both with a far-field microscope (weakly confined mode is easier to scatter by surface features) and the SNOM (the detection efficiency of a fiber probe increases for lower spatial frequencies). The fact that we could not observe the CPP guiding with groove N1 is most probably related to its shape [Fig. 3(a)]. This groove has a rather small angle (~16°) at its bottom that results in an increase of the CPP confinement and a decrease of the CPP propagation length as compared to groove 2. The first feature would make the imaging efficiency smaller (as argued above) and the second feature would drastically decrease the CPP field to be imaged.

In summary, we have modeled, realized, and characterized the CPP propagation along subwavelength-sized metal grooves. Using SNOM imaging, we have demonstrated low-loss (propagation length ~100 μm) and well-confined (mode width $\cong$ 1.1 μm) CPP guiding at telecom wavelengths (1425–1620 nm) along a triangular 0.6 μm-wide and 1 μm-deep groove in gold. Our simple model based on the effective-index method allowed us to corroborate the numerical results reported previously [12,13], determine the parameter range needed to realize the single-mode regime of CPP guiding, and account for the main features of our experiments. We believe that the fact that the CPP mode can be *both* confined to the subwavelength cross section and guided with low dissipation holds promises for low-loss large-angle splitting and bending, opening thereby a wide variety of potential applications for CPPs, from optical interconnects to biosensors.

One of the authors (S. I. B.) thanks A. A. Maradudin for fruitful discussions of SPP propagation along structured metal surfaces that led to this work. The authors acknowledge support from the European Network of Excellence, PLASMO-NANO-DEVICES (FP6-2002-IST-1-507879) and STREP SPP (FP6-NMP4-CT-2003-505699.

*Email: sergey@physics.auc.dk

[1] H. Raether, *Surface Plasmons* (Springer-Verlag, Berlin, 1988).
[2] W. L. Barnes, A. Dereux, and T. W. Ebbesen, Nature (London) **424**, 824 (2003).
[3] J. Takahara *et al.*, Opt. Lett. **22**, 475 (1997).
[4] M. Quinten, A. Leitner, J. R. Krenn, and F. R. Aussenegg, Opt. Lett. **23**, 1331 (1998).
[5] S. A. Maier *et al.*, Nat. Mater. **2**, 229 (2003).
[6] J. R. Krenn and J. C. Weeber, Phil. Trans. R. Soc. A **362**, 739 (2004).
[7] S. I. Bozhevolnyi *et al.*, Phys. Rev. Lett. **86**, 3008 (2001).
[8] K. Tanaka and M. Tanaka, Appl. Phys. Lett. **82**, 1158 (2003).
[9] B. Wang and G. P. Wang, Appl. Phys. Lett. **85**, 3599 (2004).
[10] J. Q. Lu and A. A. Maradudin, Phys. Rev. B **42**, 11159 (1990).
[11] I. V. Novikov and A. A. Maradudin, Phys. Rev. B **66**, 035403 (2002).
[12] D. F. P. Pile and D. K. Gramotnev, Opt. Lett. **29**, 1069 (2004).
[13] D. K. Gramotnev and D. F. P. Pile, Appl. Phys. Lett. **85**, 6323 (2004).
[14] E. D. Palik, *Handbook of Optical Constants of Solids* (Academic, New York, 1985).
[15] A. B. Buckman, *Guided-Wave Photonics* (Saunders College Publishing, New York, 1992).
[16] S. I. Bozhevolnyi *et al.*, J. Lightwave Technol. **23**, 413 (2005).
[17] S. I. Bozhevolnyi *et al.*, Phys. Rev. B **66**, 235204 (2002).
[18] Since the main component of the SPP electric field is oriented perpendicular to the metal surface [1], the CPP electric field tends to be oriented perpendicular to the groove walls and thereby, for small groove angles, parallel to the sample surface.